Hydration and Conformational Equilibria of Simple Hydrophobic and Amphiphilic Solutes

Henry S. Ashbaugh,* Eric W. Kaler,* and Michael E. Paulaitis#
*Department of Chemical Engineering and Center for Molecular and Engineering Thermodynamics, University of Delaware, Newark, Delaware 19716, and #Department of Chemical Engineering, The Johns Hopkins University, Baltimore, Maryland 21218 USA

ABSTRACT We consider whether the continuum model of hydration optimized to reproduce vacuum-to-water transfer free energies simultaneously describes the hydration free energy contributions to conformational equilibria of the same solutes in water. To this end, transfer and conformational free energies of idealized hydrophobic and amphiphilic solutes in water are calculated from explicit water simulations and compared to continuum model predictions. As benchmark hydrophobic solutes, we examine the hydration of linear alkanes from methane through hexane. Amphiphilic solutes were created by adding a charge of $\pm 1e$ to a terminal methyl group of butane. We find that phenomenological continuum parameters fit to transfer free energies are significantly different from those fit to conformational free energies of our model solutes. This difference is attributed to continuum model parameters that depend on solute conformation in water, and leads to effective values for the free energy/surface area coefficient and Born radii that best describe conformational equilibrium. In light of these results, we believe that continuum models of hydration optimized to fit transfer free energies do not accurately capture the balance between hydrophobic and electrostatic contributions that determines the solute conformational state in aqueous solution.

INTRODUCTION

The thermodynamics of self-assembly in aqueous solution is governed in large part by the microscopic structure and organization of water around solutes having distinct chemical architectures. Perhaps the simplest self-assembly process driven by solvent-mediated forces is the pairwise association of methane in water. Explicit water simulations have been applied extensively to characterize the methane-methane potential of mean force in water (New and Berne, 1995; Pangali et al., 1979; Smith and Haymet, 1993; van Belle and Wodak, 1993; Young and Brooks, 1997), which in turn has been useful for inferring the influence of hydrophobic interactions on the self-assembly of more complicated solutes. The effects of temperature (Lüdemann et al., 1996, 1997; Skipper et al., 1996), pressure (Hummer et al., 1998; Payne et al., 1997), and the shape of simple, idealized hydrophobic solutes (Garde et al., 1996; Wallqvist and Berne, 1995a,b) on hydrophobic interactions have been studied with this approach to provide insights into the molecular mechanisms of, for example, protein folding (Kauzmann, 1959) or surfactant self-assembly (Hunter, 1987; Israelachvili, 1992) in aqueous solution. Explicit water simulations of the hydration of simple *n*-alkanes (Garde et al., 1996; Jorgensen, 1982; Jorgensen and Buckner, 1987; Kaminski et al., 1994; Rosenberg et al., 1982; Tobias and Brooks, 1990; Wallqvist and Covell, 1995, 1996) have likewise proven useful for examining the influence of hydrophobic interactions in stabilizing certain molecular conformations in aqueous solution.

For applications involving macromolecular solutes, explicit water simulations have only limited utility because of the large number of waters of hydration and the large number of solute internal degrees of freedom that must be taken into account. The statistical precision required for these simulations places inordinate demands on computational resources and limits the system sizes that can be realized. An alternative approach is to use implicit water models, such as those embodied in continuum models of hydration. Solvent-mediated driving forces are accounted for within the context of the continuum model, but the inherent differences between water organization around hydrophobic and hydrophilic solutes lead to disconnected theoretical treatments of hydrophobic and hydrophilic hydration. For example, the hydrophobic contribution to the free energy of hydration is usually taken to be proportional to solute surface area (Chothia, 1974; Hermann, 1972; Reynolds et al., 1974), although the definition of surface area is not unique (Lee and Richards, 1971; Richards, 1977). Electrostatic contributions, on the other hand, are calculated assuming the solvent responds as a macroscopic dielectric medium on all length scales (Honig and Nicholls, 1995; Jackson, 1975; Nakamura, 1996; Rogers, 1986). Consequently, phenomenological parameters contained in the continuum model must be fit to selected experimental data. Alanine dipeptide conformational equilibria (Marrone et al., 1996; Ösapay et al., 1996; Schmidt and Fine, 1994) and self-assembly processes, such as α-helix propagation (Yang and Honig, 1995a) and β-sheet formation (Yang and Honig,

Received for publication 9 February 1998 and in final form 1 May 1998.
Address reprint requests to Dr. Michael E. Paulaitis, Department of Chemical Engineering, Johns Hopkins University, Maryland Hall 221, 3400 N. Charles St., Baltimore, MD 21218. Tel.: 410-516-7170; Fax: 410-516-5510; E-mail: michaelp@jhu.edu.

Dr. Ashbaugh's present address is Physical Chemistry 1, Center for Chemistry and Chemical Engineering, Lund University, P.O. Box 124, S-221 00 Lund, Sweden. E-mail: Hank.Ashbaugh@fkem1.lu.se.

0006-3495/98/08/755/14 $2.00

1995b), have been described successfully by using the continuum model with parameters fit to the solubilities of small nonpolar and polar solutes in water (Schmidt and Fine, 1994; Sitkoff et al., 1994, 1996). However, the physical significance of these parameters is not evident, and the consequences of applying these parameters to the description of complex self-assembly phenomena are uncertain.

Continuum model parameters can also be fit to explicit water simulations as a means of evaluating the intrinsic macroscopic approximations to "microscopic reality" in the continuum model. For example, a consequence of treating water as a macroscopic dielectric medium is that the solvent-induced electrostatic potential varies linearly with charge on the solute (Åqvist and Hansson, 1996; Figueirido et al., 1994; Pratt et al., 1994). Thus the electrostatic contribution to the hydration free energy is proportional to the square of solute charge. Extensive simulations of both ionic and polar solutes in explicit water have been carried out to test the validity of the continuum approximation, which for ion hydration is found to hold over a wide range of ionic charge (Garde et al., 1998; Hummer et al., 1996b; Jayaram et al., 1989; Kalko et al., 1996; Straatsma and Berendsen, 1988). In contrast, electrostatic interactions between polar solutes and water frequently do not exhibit a linear response (Åqvist and Hansson, 1996). In particular, when the polar solute is water itself, the solvent response is distinctly nonlinear (Hummer et al., 1995; Rick and Berne, 1994).

The central question we address in this paper is: Can the continuum model describe simultaneously the vacuum-to-water transfer free energies of simple hydrophobic and amphiphilic solutes, as well as their conformational equilibria in aqueous solution? To this end, we consider idealized hydrophobic and hydrophilic solutes at infinite dilution in water and calculate their free energies of transfer from vacuum to water, as well as the change in free energy of hydration for well-defined conformational transitions. The normal alkanes serve as benchmarks for hydrophobic hydration. We consider as well *n*-butane with a charge of $\pm 1e$ (e is the fundamental unit of charge) added to one terminal methyl group. These ionic tetramers were selected for two reasons. First, the effect of electrostatic interactions with water can be separated from the underlying hydrophobic contributions, because the hydration thermodynamics of *n*-butane has been studied extensively by simulation. Second, these solutes represent idealized models of amphiphilic molecules for which we can adjust unambiguously the balance between hydrophobic and hydrophilic interactions.

FREE ENERGY PERTURBATION USING EXPLICIT WATER SIMULATIONS

The free energy of hydration, ΔA_{hyd}, for a monatomic solute is defined as the free energy of transferring the solute from vacuum to water (Ben-Naim, 1978; Ben-Naim and Marcus, 1984). For molecular solutes, ΔA_{hyd} also depends on solute conformation, which for linear alkane chains we define by the backbone dihedral angles, $\phi = (\phi_1, \phi_2, \ldots, \phi_n)$. The probability of observing a specific solute conformation in water is dictated by $\Delta A_{\mathrm{hyd}}(\phi)$ and the intramolecular energy of this solute conformation in the ideal gas, $\Delta E_{\mathrm{int}}(\phi)$:

$$P(\phi) \propto \exp\{-\beta[\Delta A_{\mathrm{hyd}}(\phi) + \Delta E_{\mathrm{int}}(\phi)]\} \tag{1}$$

where $\beta^{-1} = k_B T$. The normalized distribution of conformations depends only on relative energy differences and not the absolute value of either $\Delta A_{\mathrm{hyd}}(\phi)$ or $\Delta E_{\mathrm{int}}(\phi)$. In this work, we neglect the intramolecular contributions and focus only on the hydration contribution; i.e., $\Delta A_{\mathrm{hyd}}(\phi)$ as a function of ϕ.

The *n*-alkane hydration free energies were calculated as the sum of hydration free energies for incrementally transforming C_{n-1} into C_n,

$$\Delta A_{\mathrm{hyd}}(C_0 \rightarrow C_n) = \sum_{i=1}^{n} \Delta A_{\mathrm{hyd}}(C_{i-1} \rightarrow C_i) \tag{2}$$

where n is the hydrocarbon chain length and C_0 denotes pure water. The $\Delta A_{\mathrm{hyd}}(C_{i-1} \rightarrow C_i)$ values are determined from the free energy perturbation (FEP) expression (Zwanzig, 1954),

$$\Delta A_{\mathrm{hyd}}(\lambda \rightarrow \lambda + \delta\lambda) = -k_B T \,\ell\mathrm{n}\langle \exp\{-\beta[E(\lambda + \delta\lambda) - E(\lambda)]\}\rangle_\lambda \tag{3}$$

where λ refers to the reference state and $\lambda + \delta\lambda$ to the perturbed state of the system, $E(\lambda)$ is the potential energy in state λ, and the brackets $\langle \ldots \rangle_\lambda$ denote averaging over solvent configurations in state λ. For the transformation $C_{i-1} \rightarrow C_i$, the Lennard-Jones (LJ) interaction parameters, σ and ϵ, of the individual methyl groups are scaled linearly with λ. This involves "growing in" the ith methyl group at a chain end and simultaneously transforming the LJ parameters of the existing groups as required by the OPLS parameterization described below, i.e., $\epsilon = \lambda\epsilon_{\mathrm{final}} + (1 - \lambda)\epsilon_{\mathrm{initial}}$ and $\sigma = \lambda\sigma_{\mathrm{final}} + (1 - \lambda)\sigma_{\mathrm{initial}}$. Perturbations of $\delta\lambda = \pm 0.05$ were performed at fixed values of λ from 0.05 to 0.95 in increments of 0.10. $\Delta A_{\mathrm{hyd}}(C_{i-1} \rightarrow C_i)$ is then calculated as the sum of $\Delta A_{\mathrm{hyd}}(\lambda \rightarrow \lambda + \delta\lambda)$ from $\lambda = 0$ to 1. These calculations were carried out for *n*-butane, *n*-pentane, and *n*-hexane in the all-*trans* conformation ($\phi = 180°$).

The free energy of hydration as a function of conformation for *n*-butane and the charged tetramers was calculated by replacing the perturbation variable λ with ϕ. The difference in hydration free energy between the *cis* ($\phi = 0°$) and *trans* ($\phi = 180°$) conformations, $\Delta A_{\mathrm{hyd}}(0° \rightarrow 180°)$, was determined at fixed values of ϕ from 7.5° to 172.5°, in increments of 15.0° with $\delta\phi = \pm 7.5°$.

The free energy of charging the ionic tetramers in water was calculated by scaling the solute charge, q_s, by λ. This free energy expanded to second order in q_s is (Hummer et

al., 1996b; Pratt et al., 1994)

$$\Delta A_{hyd}(0 \rightarrow q_s) = q_s\langle \partial E/\partial q_s\rangle_0 - \beta q_s^2/2[\langle(\partial E/\partial q_s - \langle \partial E/\partial q_s\rangle_0)^2\rangle_0 - k_B T\langle \partial^2 E/\partial q_s^2\rangle_0] \quad (4)$$

For a system that is truly infinite in size, the ion-water electrostatic energy is directly proportional to q_s multiplied by the electrostatic potential at the charge site, $\Phi \equiv \partial E/\partial q$, and $\partial^2 E/\partial q_s^2$ is zero. However, for the finite, periodic systems employed in our simulations, self-interactions arise (Hummer et al., 1996b) and must be accounted for in calculating the electrostatic energy. The self-interaction energy is quadratic in q_s, and thus $\partial^2 E/\partial q_s^2$ is nonzero.

The only difference between positive and negative ions in Eq. 4 arises from $\langle \partial E/\partial q_s\rangle_0$, the electrostatic potential at zero charge. Previous studies have shown that this quantity is positive, thereby favoring the hydration of anions (Ashbaugh and Wood, 1997; Hummer et al., 1996b, 1997; Pratt et al., 1994). The fluctuations in the electrostatic potential, however, depend strongly on the sign of q_s (Garde et al., 1998; Hummer et al., 1996b), and in Eq. 4 these fluctuations are evaluated only at zero charge. Therefore, a more accurate expression for $\Delta A_{hyd}(0 \rightarrow q_s)$, which incorporates this information at charge state q_s, is (Hummer and Szabo, 1996)

$$\begin{aligned}\Delta A_{hyd}(0 \rightarrow q_s) = {} & q_s/2(\langle \partial E/\partial q_s\rangle_0 + \langle \partial E/\partial q_s\rangle_{q_s}) \\ & - \beta q_s^2/12[\langle(\partial E/\partial q_s - \langle \partial E/\partial q_s\rangle_0)^2\rangle_0 \\ & - k_B T\langle \partial^2 E/\partial q_s^2\rangle_0 \\ & - \langle(\partial E/\partial q_s - \langle \partial E/\partial q_s\rangle_{q_s})^2\rangle_{q_s} \\ & + k_B T\langle \partial^2 E/\partial q_s^2\rangle_{q_s}]\end{aligned} \quad (5)$$

which is exact to fourth order in q_s. It should be noted that this expression requires simulation results only at the initial and final charge states to obtain an accurate estimate of $\Delta A_{hyd}(0 \rightarrow q_s)$.

Canonical ensemble Monte Carlo (MC) simulations (Allen and Tildesley, 1987) of one solute molecule at infinite dilution in water were performed at a temperature of 25°C and a water density of 0.997 g/cm^3. The details of these simulations are given in Table 1. Water was modeled using the simple point charge (SPC) potential (Berendsen et al., 1981). The *n*-alkanes were modeled using the OPLS united-atom LJ potential parameters (Jorgensen et al.,

TABLE 1 Conditions and simulation lengths for the free energy determinations. All simulations were conducted at 25°C with one solute molecule at infinite dilution in N_w water molecules.

n-Alkane solubility simulations. Ten simulations between the initial and final solute states were performed, holding λ fixed at values from 0.05 to 0.95.

Simulation*	N_w	Volume# (Å^3)	No. of equilibration passes per λ§	No. of sampling passes per λ§
$C_0 \rightarrow C_1$	216	6518	40,000	200,000
$C_1 \rightarrow C_2$	216	6569	40,000	200,000
$C_2 \rightarrow C_3$	216	6598	40,000	200,000
$C_3 \rightarrow C_4$	216	6628	40,000	200,000
$C_4 \rightarrow C_5$	216	6658	40,000	200,000
$C_5 \rightarrow C_6$	216	6687	40,000	200,000

Charging simulations for the terminal carbon of *trans*-butane

Simulation	N_w	Volume¶ (Å^3)	No. of equilibration passes§	No. of sampling passes
C_4	212	6522	40,000	160,000
C_4 ($q_s = +1e$)	212	6522	40,000	160,000
C_4 ($q_s = -1e$)	212	6522	40,000	160,000

Cis to *trans* conformational free energy simulations of uncharged and charged butane. Twelve simulations between the initial and final conformational states were performed, holding ϕ fixed at values ranging from 7.5° to 172.5°.

Simulation	N_w	Volume¶ (Å^3)	No. of equilibration passes per ϕ**	No. of sampling passes per ϕ**
C_4 ($\phi = 0° \rightarrow 180°$)	212	6522	40,000	160,000
C_4^+ ($\phi = 0° \rightarrow 180°$)	212	6522	40,000	160,000
C_4^- ($\phi = 0° \rightarrow 180°$)	212	6522	40,000	160,000

*As stated in the text, the alkane chains were grown into solution one alkyl site at a time in the all-*trans* conformation. The notation $C_n \rightarrow C_{n+1}$ denotes a simulation in which an alkane *n* carbon groups long is transformed into an alkane $n + 1$ carbon groups long.

#The volume of the simulation cell is obtain from the partial molar volume of water ($\bar{v}_w = 30.0$ Å^3) and the neat liquid alkane densities. For a $C_n \rightarrow C_{n+1}$ transformation, the average partial molar volume of the initial and final solutes was used.

§One MC pass is equal to four attempted solute moves and N_w attempted solvent moves.

¶A partial molar volume of 162 Å^3 is assumed for both *n*-butane and ionic tetramers.

**One MC pass is equal to one attempted solute move and N_w attempted solvent moves for the conformational simulations. Preferential sampling was employed to enhance solvent moves in the vicinity of the solute (Owicki and Scheraga, 1977).

1984). Solute-water cross-interaction parameters were obtained from the geometric mean combining rules, i.e., $\sigma_{sw} = (\sigma_{ss}\sigma_{ww})^{1/2}$ and $\epsilon_{sw} = (\epsilon_{ss}\epsilon_{ww})$. Potential and structural parameters for water and the *n*-alkanes are given in Table 2. LJ parameters for the charged tetramers were assumed to be the same as those for uncharged *n*-butane. Minimum image LJ interactions were truncated on a site-by-site basis at half the simulation box length, $L/2$. Solute perturbations and averages were evaluated on the fly once every MC pass (see Table 1). Statistical uncertainties in the free energy were estimated from block averages obtained by dividing the simulation runs into five equal blocks that were assumed to be independent.

Electrostatic interactions were evaluated by the generalized reaction-field (GRF) method (Hummer et al., 1994). Although Ewald summation (De Leeuw et al., 1980) is generally regarded as the best available technique for calculating the electrostatic energy of a periodic system of charges, the method is slowed by the calculation of long-range Fourier space contributions. The GRF method, on the other hand, neglects long-range contributions to the energy and therefore can be evaluated more rapidly. Previous simulation studies have shown that the two methods give essentially the same pair correlation structure of aqueous electrolyte solutions (Hummer et al., 1994, 1996b). Most importantly, the two methods give identical charging free energies of both ionic (Hummer et al., 1996b) and polar solutes (Hummer et al., 1995).

TABLE 2 Interaction parameters and geometrical constraints of simulated water* and the *n*-alkanes#

Lennard-Jones and electrostatic interaction parameters			
Molecular site	σ (Å)	ϵ (kcal/mol)	q (e)
Methane, CH_4	3.730	0.294	0.0
Ethane, CH_3	3.775	0.207	0.0
Propane and longer alkanes			
Terminal carbon, CH_3	3.905	0.175	0.0 (or ± 1 e for butane)
Interior carbon, CH_2	3.905	0.118	0.0
SPC water			
Oxygen	3.16557	0.1554	−0.82
Hydrogen	0.0	0.0	+0.41

Intramolecular bond lengths	
Bond	r (Å)
Alkanes	
C-C	1.53
SPC water	
O-H	1.00

Intramolecular angles	
Angle	(degrees)
Alkanes	
$C_i - C_{i+1} - C_{i+2}$	109.47°
SPC water	
H-O-H	109.47°

* See Berendsen et al. (1981).
#See Jorgensen et al. (1984).

The GRF electrostatic energy of a system of N_w water molecules and one solute molecule is

$$\begin{aligned} E_{GRF} = & \sum_{1\le i<j\le N_w} \sum_{\alpha=1}^{3} \sum_{\beta=1}^{3} q_{w_\alpha} q_{w_\beta} \varphi_{GRF}(r_{i_\alpha j_\beta}) \\ & + \sum_{i=1}^{N_w} \sum_{\alpha=1}^{\nu} \sum_{\beta=1}^{3} q_{s_\alpha} q_{w_\beta} \varphi_{GRF}(r_{s_\alpha j_\beta}) \\ & + 1/2 \sum_{i=1}^{N_w} \sum_{\alpha=1}^{3} \sum_{\beta=1}^{3} q_{w_\alpha} q_{w_\beta} \psi_{GRF}(r_{i_\alpha i_\beta}) \\ & + 1/2 \sum_{\alpha=1}^{\nu} \sum_{\beta=1}^{\nu} q_{s_\alpha} q_{s_\beta} \psi_{GRF}(r_{s_\alpha s_\beta}) \end{aligned} \tag{6}$$

where q_{w_α} and q_{s_α} are the water and solute partial charges, and ν is the number of solute charge sites. A factor of $1/4\pi\epsilon_0$ is neglected in Eq. 6 for notational simplicity, where ϵ_0 is the permittivity of free space. The effective GRF electrostatic pair potential depends only on the minimum image distance r between charges and has a cutoff distance r_c:

$$\begin{aligned} \varphi_{GRF}(r) = & \, 1/r(1 - r/r_c)^4(1 + 8r/5r_c + 2r^2/5r_c^2) \\ & \times \Theta(r_c - r) - \pi r_c^2/5L^3 \end{aligned} \tag{7}$$

where $\Theta(x)$ is the Heaviside unit-step function. The self-interaction potential is defined as (Hummer et al., 1995, 1996b) $\psi_{GRF}(r) = \varphi_{GRF}(r) - 1/r$. An electrostatic cutoff of $r_c = L/2$ is used throughout this work.

For a solute with one charge site ($\nu = 1$), the derivatives of the electrostatic energy with respect to q_s are

$$\partial E/\partial q_s = \Phi_{GRF} + q_s \psi_{GRF}(0) \tag{8a}$$

and

$$\partial^2 E/\partial q_s^2 = \psi_{GRF}(0) \tag{8b}$$

where

$$\Phi_{GRF} = \sum_{i=1}^{N_w} \sum_{\alpha=1}^{3} q_{w_\beta} \varphi_{GRF}(r_{N j_\alpha}) \tag{8c}$$

Φ_{GRF} is the direct GRF electrostatic potential at the solute charge site due to the solvent water molecules. $\psi_{GRF}(0)$ corrects for finite system size and potential cutoff effects on the electrostatic energy. For $r_c = L/2$, the GRF self-interaction term is $\psi_{GRF}(0) = -24/5L - \pi/20L$. In the limit of an infinite simulation size, it is easily confirmed that $\psi_{GRF}(0) = 0$ and Φ_{GRF} corresponds to the true $1/r$ electrostatic potential. Inclusion of the self-interaction energy makes the free energy of charging an ion robust such that the limiting infinite dilution value is approached for simulations of moderate size ($N_w > 64$) without further correction (Hummer et al., 1996b).

CONTINUUM MODEL OF HYDRATION

The thermodynamic cycle employed by the continuum model to calculate ΔA_{hyd} is depicted in Fig. 1. In the first step the solute charges are turned off in vacuum, ΔA_{vac} ($q_s \rightarrow 0$). In the second step the uncharged solute is transferred from the vacuum to the condensed aqueous phase, $\Delta A_{H\Phi}$. Finally, the solute charges are turned back on in solution, $\Delta A_{aq}(0 \rightarrow q_s)$. The work required to perform all three steps is the hydration free energy,

$$\Delta A_{hyd} = \Delta A_{vac}(q_s \rightarrow 0) + \Delta A_{H\Phi} + \Delta A_{aq}(0 \rightarrow q_s) \qquad (9)$$

The individual contributions to ΔA_{hyd} are evaluated as follows.

The free energy of transferring *n*-alkanes (excluding methane) from vacuum to water is found empirically to be linear with the molecular surface area of the solute (Hermann, 1972; Chothia, 1974; Reynolds et al., 1974). This observation suggests the following expression for hydrophobic contributions to the free energy of hydration (step 2 in Fig. 1):

$$\Delta A_{H\Phi} = \gamma \mathcal{A} + b \qquad (10)$$

where $\mathcal{A}$ is solute surface area, γ is the free energy/surface area coefficient, and b is the free energy intercept. The free energy/surface area coefficient is frequently referred to as a surface tension, although its connection to a macroscopic oil/water surface tension is merely anecdotal. Several definitions of solute surface area have been proposed: the van der Waals (vdW), solvent-accessible (SAS), and molecular surface areas. Differences between these definitions are discussed in detail elsewhere (Lee and Richards, 1971; Richards, 1977). All three surface areas were calculated using Connolly's Molecular Surface Program (Connolly, 1981, 1983) and a methyl/methylene group vdW radius of 1.9 Å and a water probe radius of 1.4 Å.

To evaluate the electrostatic contributions to the free energy (steps 1 and 3 of Fig. 1), the solute is treated as a low dielectric cavity imbedded within a high dielectric solvent (water) or in a vacuum. The resulting Poisson equation (Jackson, 1975) for the electrostatic potential is

$$\nabla^2 \Phi_i(\mathbf{r}) = -\frac{\sum_{\alpha=1}^{\nu} q_{s_\alpha} \delta(\mathbf{r} - \mathbf{r}_\alpha)}{\epsilon_i \epsilon_0} \qquad \mathbf{r} \in B_i \qquad (11a)$$

and

$$\nabla^2 \Phi_e(\mathbf{r}) = 0 \qquad \mathbf{r} \in B_e \qquad (11b)$$

where $\mathbf{r}$ is the spatial coordinate, Φ_i and Φ_e are the electrostatic potentials in the interior and exterior regions of the solute denoted by B_i and B_e respectively, ϵ_i is the dielectric constant of the solute interior, ν is the number of interior solute charges, $\{\mathbf{r}\}$ is the set of charge positions, and $\delta(\mathbf{r})$ is the Dirac delta function. Φ_i and Φ_e are subject to the following boundary conditions at the solute/solvent interface:

$$\Phi_i(\mathbf{r}) = \Phi_e(\mathbf{r}) \qquad \mathbf{r} \in \partial B \qquad (12a)$$

and

$$\epsilon_i \frac{\partial \Phi_i(\mathbf{r})}{\partial n} = \epsilon_e \frac{\partial \Phi_e(\mathbf{r})}{\partial n} \qquad \mathbf{r} \in \partial B \qquad (12b)$$

where ∂B denotes the interfacial surface bordering regions B_i and B_e, ϵ_e is the dielectric constant of the solvent, and $\partial/\partial n$ is the derivative with respect to the outward unit surface normal of ∂B.

Poisson's equation must be solved numerically for polyatomic solutes. This is accomplished by using the boundary element method (BEM) to solve the surface integral form of Poisson's equation for Φ_i and $\partial \Phi_i/\partial n$ on ∂B (Horvath et al., 1996; Pratt et al., 1997; Rashin, 1990; Yoon and Lenhoff, 1990; Zauhar and Morgan, 1985). The electrostatic potential at a position $\mathbf{r}$ in the solute interior is then obtained from

$$\Phi_i(\mathbf{r}) = 1/4\pi\epsilon_i\epsilon_0 \sum_{\alpha=1}^{\nu} \frac{q_{s_\alpha}}{|\mathbf{r} - \mathbf{r}_\alpha|} + \Phi_{surf}(\mathbf{r}) \qquad (13a)$$

where

$$\Phi_{surf}(\mathbf{r}) = \frac{1}{4\pi\epsilon_0} \int_{\partial B} \left[\frac{\partial \Phi_i(\mathbf{r}')}{\partial n} \frac{1}{|\mathbf{r} - \mathbf{r}'|} - \Phi_i(\mathbf{r}') \frac{\partial}{\partial n} \left(\frac{1}{|\mathbf{r} - \mathbf{r}'|} \right) \right] d\mathcal{A}(\mathbf{r}') \qquad (13b)$$

and $d\mathcal{A}(\mathbf{r}')$ is a differential area element of the solute surface at $\mathbf{r}' \in \partial B$. The first term on the right-hand side of Eq. 13a is due to the direct electrostatic interactions with the interior solute charges, and $\Phi_{surf}(\mathbf{r})$ is the solvent contribution to the potential arising at the solute surface. The electrostatic free energy of transferring the solute from vacuum

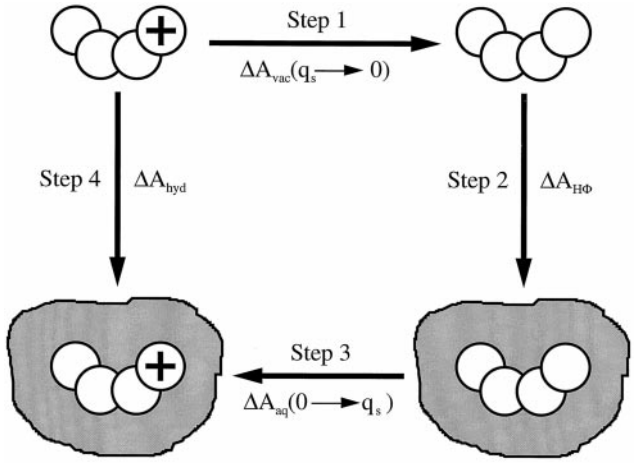

FIGURE 1 The thermodynamic path used to evaluate the hydration free energy of a charged solute in a fixed conformation.

to aqueous solution is

$$\Delta A_{\text{elec}} = 1/2 \sum_{\alpha=1}^{\nu} q_{s_\alpha}[\Phi_{\text{surf}}(\mathbf{r}_\alpha, \epsilon_e = \epsilon_{aq}) - \Phi_{\text{surf}}(\mathbf{r}_\alpha, \epsilon_e = 1)] \quad (14)$$

where $\Delta A_{\text{elec}} = \Delta A_{\text{vac}}(q_s \rightarrow 0) + \Delta A_{\text{aq}}(0 \rightarrow q_s)$, ϵ_{aq} is the dielectric constant of water, and $\epsilon_e = 1$ is the dielectric constant of a vacuum. ϵ_i is assumed to be equal to 1 because the simulations neglect molecular polarizability. In this case there is no dielectric discontinuity at the solute boundary in a vacuum and $\Delta A_{\text{vac}}(q_s \rightarrow 0)$ is zero. ϵ_{aq} is set equal to 65, the dielectric constant of SPC water at ambient conditions (Hummer et al., 1995, 1996b). For large ϵ_e the continuum free energy is insensitive to the value of ϵ_e.

For a spherical ion in solution, Poisson's equation can be solved analytically. In this case, the charging free energy is given by the Born equation (Born, 1920):

$$\Delta A_{\text{elec}} = -q_s^2/8\pi\epsilon_0 R(1 - 1/\epsilon_{aq}) \quad (15)$$

where R is the Born radius of the ion. The Born radius is typically treated as an adjustable parameter that reflects the effects of water structure in the vicinity of the ion. We model the molecular solutes as a collection of spheres with Born radii that depend on the final charge of each carbon site. The radius of an uncharged methyl/methylene group, R_0, is taken to be the vdW radius, 1.9 Å. The Born radii of positively (R_+) and negatively (R_-) charged methyl groups are fit to free energies obtained from explicit water simulations. The solute interior, B_i, is defined by the molecular surface (Richards, 1977), which is calculated by rolling a 1.4-Å-radius probe over the Born radii of the solute in a given conformation.

The surface discretization of ∂B was performed using Zauhar's SMART (Smooth MoleculAR Triangulator) program (Zauhar, 1995). Rather than approximating each triangluar surface element as flat, this algorithm generates a more accurate curvilinear representation of the solute surface. An angle parameter of 25° was used to triangulate the solute molecular surface (Zauhar, 1995). Using a finer element size did not affect the results significantly. The SMART discretized surface was input into the BEM Poisson solver developed by Neal and Lenhoff (Neal, 1997). Φ_i and $\partial\Phi_i/\partial n$ were assumed to vary linearly over each element, and the surface integrals were evaluated using Gaussian quadrature.

RESULTS AND DISCUSSION

n-Alkanes in aqueous solution

The calculated *n*-alkane free energies of hydration in SPC water are reported in Table 3. Previously reported simulation results for TIP4P water (Kaminski et al., 1994) and experimental values from the literature (Ben-Naim and Marcus, 1984; McAuliffe, 1966) are also included in this table. Not surprisingly, ΔA_{hyd} is positive for all of the *n*-alkanes, indicative of their low solubilities in water. The free energies obtained from the SPC water simulations are in very good agreement with those calculated from the TIP4P water simulations. The simulations also predict, in accord with experiment, that ΔA_{hyd} decreases from methane to ethane, but then increases with increasing carbon number for longer *n*-alkanes. However, the simulations significantly overestimate the experimental values of ΔA_{hyd}. The disparities between simulations and experiment are due in large part to the discrepancy in the incremental free energy of adding a methylene group to ethane: $\Delta A_{\text{hyd}}(C_2 \rightarrow C_3)$ is 0.21 kcal/mol from experiment and 0.73 ± 0.04 kcal/mol from the SPC water simulations. Differences between simulation and experiment also occur to some extent as a consequence of systematic differences in the OPLS united-atom parameters for methane, ethane, and propane (Table 2). For propane and the longer *n*-alkanes, the united-atom parameters are independent of chain length. Consequently, the incremental free energy of hydration of adding a methylene group to these alkane chains obtained from simulation is approximately constant (~0.2 kcal/mol) and is in good agreement with experiment. Plotting the cumulative values of $\Delta A_{\text{hyd}}(C_{i-1} \rightarrow C_i)$ as a function of λ clearly illustrates this behavior (Fig. 2). The incremental free energy profiles for methane, ethane, and propane (i = 1, 2, 3) show little resemblence to one another. However, for *n*-butane, *n*-pentane, and *n*-hexane (i = 4, 5, 6), these profiles are practically indistinguishable.

TABLE 3 Free energies and incremental free energies of hydration of the *n*-alkanes in water at 25°C

Solute	SPC*	ΔA_{hyd} ($C_{i-1} \rightarrow C_i$) TIP4P#	Expt§	SPC*	ΔA_{hyd} TIP4P#	Expt§
C_1	2.62 (0.11)	2.46 (0.36)	1.93	2.62 (0.11)	2.46 (0.36)	1.93
C_2	−0.05 (0.05)	−0.13 (0.20)	−0.16	2.57 (0.12)	2.33 (0.41)	1.77
C_3	0.73 (0.04)	0.98 (0.10)	0.21	3.30 (0.13)	3.31 (0.42)	1.98
C_4	0.21 (0.05)	0.27 (0.17)	0.17	3.51 (0.13)	3.58 (0.46)	2.15
C_5	0.18 (0.05)	—	0.19	3.69 (0.14)	—	2.34
C_6	0.23 (0.05)	—	0.21	3.92 (0.15)	—	2.55

The units of free energy are kcal/mol. Numbers in parentheses are the statistical uncertainties reported as one standard deviation.

*SPC water simulations from this work with the solutes in the all-*trans* conformation. The LJ interactions were corrected to give the same effective solute-water potential cut-off of 9 Å for all alkanes, assuming the radial distribution function is equal to 1 far away from the solute.

#TIP4P water simulations (Kaminski et al., 1994). Results are not reported for C_5 and C_6.

§Values obtained from experimental *n*-alkane solubilities in water (Ben-Naim and Marcus, 1984; McAuliffe, 1966).

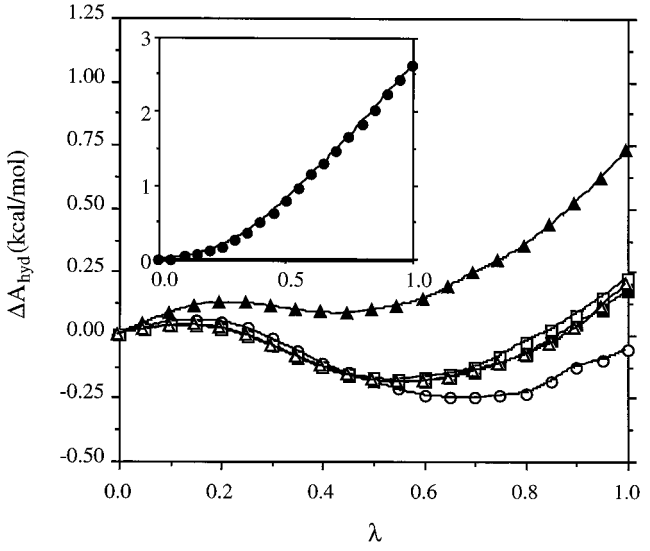

FIGURE 2 Cumulative values of $\Delta A_{hyd}(C_{i-1} \rightarrow C_i)$ as a function of λ. Symbols correspond to $i = 1$ (●), $i = 2$ (○), $i = 3$ (▲), $i = 4$ (△), $i = 5$ (■), and $i = 6$ (□). Results for $i = 1$ are plotted in the inset.

Free energies of hydration are plotted as a function of *n*-alkane SAS area in Fig. 3. Excluding methane, the experimental values show a linear dependence on SAS area. A linear regression of the data gives $\gamma_{SAS}^{expt} = 6.8$ cal/(mol Å^2) and $b_{SAS}^{expt} = 0.6$ kcal/mol. The values obtained from simulation do not show the same linear dependence below the SAS area for propane, which can be attributed to the systematic differences in the OPLS united-atom parameters

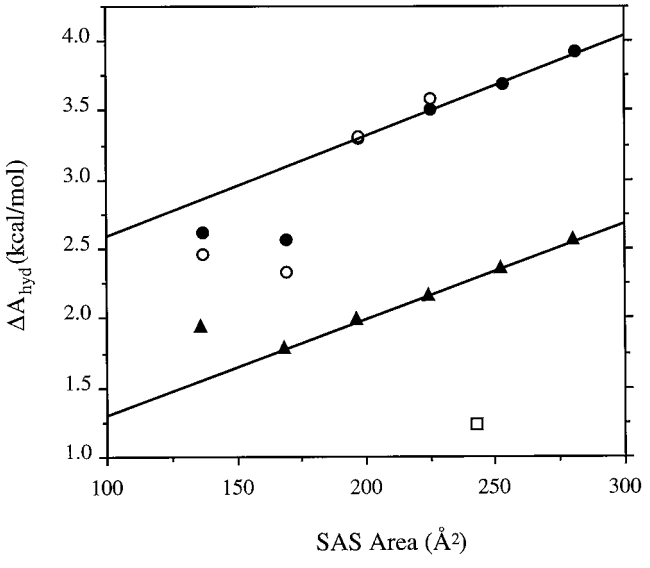

FIGURE 3 ΔA_{hyd} as a function of *n*-alkane SAS area. ●, The SPC water simulation results from this work. ○, TIP4P water simulation results (Kaminski et al., 1994). ▲, Experimental values (Ben-Naim and Marcus, 1984; McAuliffe, 1966). The solid lines are the best fits of Eq. 10 to the results for the longer chain alkanes. The line through the experimental data is $\Delta A_{hyd} = 6.8$ cal/(mol Å^2)$\mathcal{A} + 0.6$ kcal/mol, and the line through the simulation data is $\Delta A_{hyd} = 7.4$ cal/(mol Å^2)$\mathcal{A} + 1.8$ kcal/mol. □, The experimental value for ΔA_{hyd} of cyclohexane.

discussed above. For the simulation results, $\gamma_{SAS}^{sim} = 7.4$ cal/(mol Å^2) and $b_{SAS}^{sim} = 1.8$ kcal/mol, which is obtained by fitting SAS areas for propane and the longer chain alkanes. Free energies of hydrophobic hydration are typically correlated with solute SAS area (Chothia, 1974; Hermann, 1972; Reynolds et al., 1974; Schmidt and Fine, 1994; Sitkoff et al., 1994, 1996). The vdW surface area or the molecular surface area could be used as well. Indeed, all three surface areas correlate linearly with ΔA_{hyd} equally well, which is not surprising, because all three surfaces are linearly correlated with each other for the *n*-alkanes. The calculated values of γ and b for the three surface areas are given in Table 4. In each case, the value of γ obtained from simulation is somewhat greater than the experimental value. Apart from the approximate nature of the intermolecular interactions used in the simulations, a major difference between simulation and experiment is the constraint of fixed all-*trans* conformation for the *n*-alkanes imposed on the simulations. The experimental results, on the other hand, are naturally averaged over all available conformations. The value of γ will not change appreciably, however, if the simulation constraint is relaxed to sample more compact conformations with lower surface areas, because the maximum change in solute surface area for the allowed conformational changes is small compared to the total area. For example, the SAS area of *n*-butane in the *cis* and *trans* conformations differs by only 4%.

Conformational free energy of *n*-butane

The simulation results for $\Delta A_{hyd}(\phi)$ as a function of *n*-butane conformation are shown in Fig. 4. The increase in $\Delta A_{hyd}(\phi)$ with increasing ϕ indicates that hydration destabilizes the elongated *trans* conformation of *n*-butane relative to the more compact *cis* conformation. This behavior is consistent with the notion that hydrophobic interactions tend to minimize the extent of oil-water contact. The $\Delta A_{hyd}(\phi)$ profiles are also in qualitative agreement with previous simulation (Jorgensen, 1982; Jorgensen and Buckner, 1987; Kaminski et al., 1994; Rosenberg et al., 1982; Tobias and Brooks, 1990) and theoretical (Hummer et al.,

TABLE 4 Values of γ and b (Eq. 10) for the *n*-alkanes in water calculated from SPC water simulations and from experimental values for *n*-alkane solubilities in water

	Simulation*		Experiment#	
Surface	γ	b	γ	b
van der Waals	12	2.3	11	1.1
Solvent-accessible	7.4	1.8	6.8	0.6
Molecular	12	2.3	12	1.0

Simulation results were fit to the C_3 through C_6 alkanes, and the experimental results were fit to the C_2 through C_6 alkanes. The units of γ are cal/(mol Å^2). The units of b are kcal/mol.

*This work with the solutes in the all-*trans* conformation.

#Values obtained from experimental *n*-alkane solubilities in water (Ben-Naim and Marcus, 1984; McAuliffe, 1966).

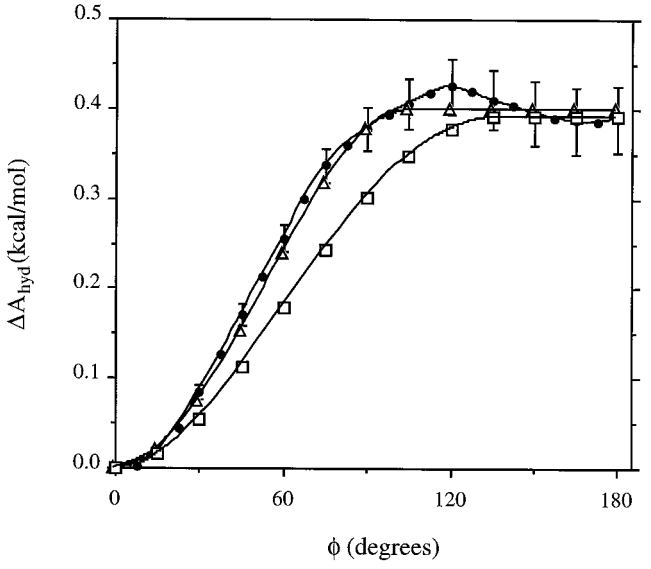

FIGURE 4 ΔA_{hyd} as a function of *n*-butane conformation referenced to $\Delta A_{hyd}(0°) = 0$. ●, SPC water simulation results. △, The fit of Eq. 10 to the simulation results, using the vdW surface (γ = 109 cal/(mol Å^2)). □, The fit of Eq. 10, using the SAS area (γ = 49.3 cal/(mol Å^2)). Error bars on the simulation results denote one standard deviation.

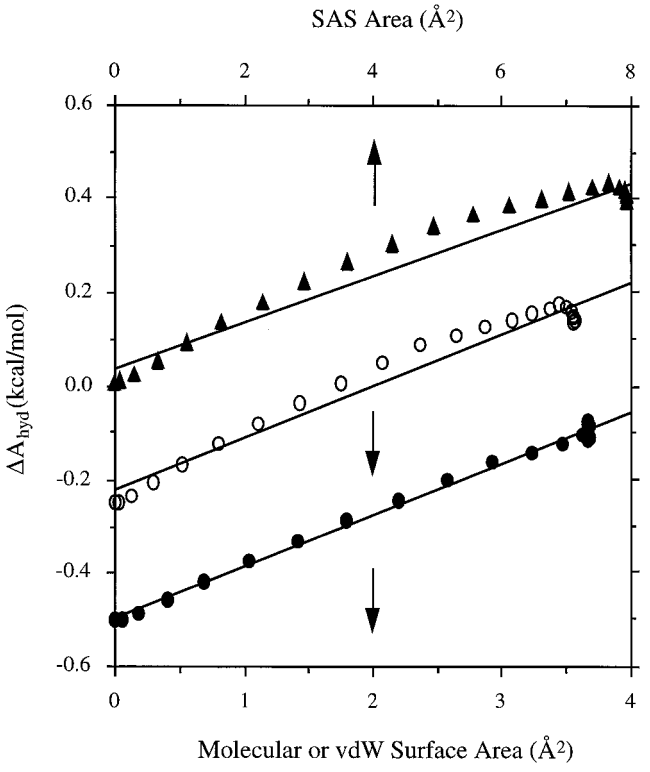

FIGURE 5 ΔA_{hyd} as a function of *n*-butane conformation as correlated with solute surface area referenced to $\mathcal{A}(0°) \equiv 0$ (*cis* conformation). ●, vdW surface area (γ = 109 cal/(mol Å^2)); ○, molecular surface area (γ = 111 cal/(mol Å^2)); ▲, SAS area (γ = 49.3 cal/(mol Å^2)). The plots for molecular surface and vdW surface areas are shifted down by 0.25 and 0.5 kcal/mol, respectively, from the plot for SAS area. The root mean square difference between the simulation results and the linear fit of Eq. 10 are 0.01, 0.03, and 0.03 kcal/mol for the vdW, solvent-accessible, and molecular surfaces, respectively.

1996a; Pratt and Chandler, 1977; Zichi and Rossky, 1986) studies of the free energy of hydration of different *n*-butane conformations in water. In Fig. 5, $\Delta A_{hyd}(\phi)$ is plotted as a function of *n*-butane surface area rather than the backbone dihedral angle. All three surface area correlations show qualitatively a linear dependence of ΔA_{hyd} on surface area, as suggested by Eq. 10. We calculate γ = 109, 49.3, and 111 cal/(mol Å^2) for the vdW, solvent-accessible, and molecular surfaces, respectively. The vdW surface area correlation gives the best fit of the simulation results based on root mean square difference (see Fig. 5). The vdW surface area correlation also captures most accurately the plateau in ΔA_{hyd} as a function of ϕ for $\phi > 90°$ (Fig. 4). The other two surface area correlations give plateaus closer to ϕ = 180° (*trans* conformation). See, for example, the fit of Eq. 10 to the simulation results, using the SAS area in Fig. 4. The success of the vdW surface area correlation is surprising in light of recent studies indicating that the molecular surface area best describes the hydrophobic interactions between methane pairs in water (Jackson and Sternberg, 1993, 1994; Pitarch et al., 1996; Rank and Baker, 1997). Interestingly, the suggested value of γ for methane-methane pair interactions, calculated using the molecular surface area, lies between 104 and 110 cal/(mol Å^2), in very good agreement with the γ value for the molecular surface area correlation in Fig. 5.

The values of γ extracted from the *n*-alkane free energies of hydration (Table 4) are an order of magnitude less than the values extracted from fits of ΔA_{hyd} as a function of *n*-butane surface area (Fig. 5), regardless of how solute surface area is defined. The justification for surface area scaling of the free energy embodied in Eq. 10 is based on the expectation that the free energy of forming a macroscopic surface scales with its surface area. It is not evident, however, that this scaling should also hold for molecular length scales, such as those associated with the surface areas of simple linear alkanes. Previous simulation studies of *n*-butane in water have shown that the entropy of hydrophobic hydration per water molecule depends on solute conformation (Ashbaugh and Paulaitis, 1996). Simulation studies of the hydration of idealized spherical and ellipsoidal solutes have likewise shown that differences between surface area derivatives of the hydration free energy could be reconciled only if solute curvature was taken into account (Wallqvist and Berne, 1995b). These results suggest that surface area scaling breaks down for molecular length scales.

Experimental evidence for this breakdown can be found by comparing values of ΔA_{hyd} derived from the measured solubilities of cycloalkanes in water to those derived from the solubilities of their *n*-alkane counterparts. The cycloalkanes can be thought of in this comparison as "collapsed" linear analogs of the *n*-alkanes constrained to ring-forming conformations. ΔA_{hyd} = 0.80, 1.20, and 1.20 kcal/mol at

25°C for cyclopropane, cyclopentane, and cyclohexane (Horvath et al., 1996), respectively. These values are much less than ΔA_{hyd} for ethane (Table 3), even though ethane is the most soluble *n*-alkane and has a lower surface area than the cycloalkanes. Moreover, as shown in Fig. 3, ΔA_{hyd} for cyclohexane falls well below the linear correlation for experimental hydration free energies of the *n*-alkanes. Based on the experimental ΔA_{hyd} and calculated SAS area differences betweeen *n*-hexane and cyclohexane, γ is 34 cal/(mol Å^2). This free energy/surface area coefficient is much closer in magnitude to the value we would calculate from the conformational equilibria. Similar conclusions can be reached for the other cycloalkanes.

We propose the following generalization of Eq. 10 to explain the large differences in free energy/surface area coefficients derived from hydration free energies and from conformational equilibria. The reversible work required to form a hydrophobic surface in water is equal to γA, where γ is the free energy/surface area coefficient calculated from *n*-alkane free energies of hydration as a function of solute surface area (Table 4). The change in the free energy of hydration associated with a conformational change for *n*-butane is given by

$$\partial(\gamma \mathcal{A})/\partial\phi = \gamma \partial \mathcal{A}/\partial\phi + \mathcal{A}\partial\gamma/\partial\phi \qquad (16)$$

The first term on the right-hand side of this equation is related to the change in hydration free energy due to a change in solute surface area. The second term reflects the change in hydration as a function of solute conformation. The free energy/surface area coefficient evaluated from conformational equilibria is simply

$$\Gamma = \partial(\gamma \mathcal{A})/\partial\phi \times \partial\phi/\partial \mathcal{A} = \gamma + \mathcal{A}\partial\gamma/\partial\mathcal{A} \qquad (17)$$

Thus the two free energy/surface area coefficients are equivalent when $\partial\gamma/\partial\mathcal{A} = 0$. However, when $\partial\gamma/\partial\mathcal{A} \neq 0$, Γ and γ can be substantially different, even if $\partial\gamma/\partial\mathcal{A}$ is small, because the second term in Eq. 17 is this derivative multiplied by the total solute area, a comparatively large quantity. Based on the vdW surface values (γ = 12.0 cal/(mol Å^2), Γ = 109 cal/(mol Å^2), and $\mathcal{A}$ = 98.1 Å^2), we estimate that $\partial\gamma/\partial\mathcal{A}$ = 1.0 cal/(mol Å^4). Thus γ varies from 8.3 cal/(mol Å^2) for *cis n*-butane to 12.0 cal/(mol Å^2) for *trans n*-butane.

Free energy of charging *trans*-butane

The simulation averages for the electrostatic potential and fluctuations in the electrostatic potential required to calculate the free energy of charging the terminal methyl group of *trans*-butane are reported in Table 5. From Eq. 5, $\Delta A_{hyd}(0e \rightarrow +1e) = -56.8 \pm 0.8$ kcal/mol and $\Delta A_{hyd}(0e \rightarrow -1e) = -94.8 \pm 1.1$ kcal/mol. Based on averages for the electrostatic potential and fluctuations in the electrostatic potential recently reported for simulations of charging methane in SPC water (Hummer et al., 1996b), we calculate $\Delta A_{hyd}(0e \rightarrow +1e) = -60.3$ kcal/mol and $\Delta A_{hyd}(0e \rightarrow -1e) = -106.6$ kcal/mol, using Eq. 5. The free energies of charging methane are slightly more negative, as expected, because the major contribution to the free energy is the electrostatic interaction with water molecules in the first hydration shell of the ion. Methane has more water molecules in its first hydration shell than does the terminal methyl group of *n*-butane, because of the excluded volume of the attached propyl group for the latter. In both cases, the free energy of charging the anion is considerably more negative than that for the cation.

TABLE 5 Simulation averages required to calculate the free energy of charging the terminal methyl group of *trans*-butane with Eq. 5

q_s	$0e$	$+1e$	$-1e$
$\langle \partial E/\partial q_s \rangle_{q_s}$	8.4 (0.4)	−123.9 (0.7)	188.6 (2.0)
$\langle (\partial E/\partial q_s - \langle \partial E/\partial q_s \rangle_{q_s})^2 \rangle_{q_s} - k_B T \langle \partial^2 E/\partial q_s^2 \rangle_{q_s}$	78.6 (1.4)	85.2 (5.1)	105.0 (3.3)

The units of electrostatic potential are kcal/(mol *e*). The numbers in parentheses are the statistical uncertainties reported as one standard deviation.

The difference in anion and cation hydration can be assigned in part to the nonzero electrostatic potential at zero charge: $\langle \partial E/\partial q_s \rangle_0 = 8.4 \pm 0.4$ kcal/(mol *e*) (Table 5). Subtracting $q_s \langle \partial E/\partial q_s \rangle_0$ from ΔA_{hyd} effectively removes this contribution from the total free energy of charging, which reduces the asymmetry in ion hydration: $q_s \langle \partial E/\partial q_s \rangle_0$ accounts for 10–15% of the total free energy of charging these ions.[1] Nonetheless, the difference is still significant: -65.2 ± 0.8 kcal/mol and -86.4 ± 1.1 kcal/mol for charging the cation and the anion, respectively. This remaining difference is due in large part to differences in the microscopic structure of water around oppositely charged ions, which is a manifestation of the asymmetrical spatial distribution of charges in the water molecule. That is, anion hydration is favored over cation hydration because the positively charged hydrogens of water molecules in the first hydration shell can reside closer to the anion than can the negatively charged oxygens of water molecules in the first hydration shell of the cation (Garde et al., 1998; Hummer et al., 1996b).

The Born radii for the charged methyl groups obtained by fitting the unadjusted free energies (i.e., those including a nonzero value of $\langle \partial E/\partial q_s \rangle_0$) are $R_+ = 2.82$ Å and $R_- = 1.56$ Å, which are in reasonable agreement with the Born radii obtained for charged methane: $R_+ = 2.71$ Å and $R_- = 1.54$ Å. The larger R_+ relative to R_- is consistent with the asymmetry in ion hydration attributed above to water structure. A consequence of assuming that the solvent responds as a macroscopic dielectric is that the free energy of charging is proportional to q_s^2 and therefore is independent of the sign of q_s (e.g., Eq. 15). Hence $\langle \partial E/\partial q_s \rangle_0$ from the continuum model must necessarily be equal to zero by symmetry to charge reversal. A more appropriate comparison between the simulation results and the continuum model would be to evaluate the Born radii from free energies with this contribution removed. We obtain $R_+ = 2.42$ Å and $R_- = 1.74$ Å

for the charged methyl groups of *n*-butane, and show below that these values yield better descriptions of the conformational equilibria of the charged tetramers than do the original, unadjusted values of the Born radii.

Conformational free energy of the charged tetramers

We expect a significant shift in the *cis-trans* conformational equilibrium of *n*-butane when a terminal methyl group is charged. The simulation results in Fig. 6 confirm this expectation. For both charged tetramers, the hydration free energy is lower for the extended *trans* conformation. This is in contrast to uncharged *n*-butane, where the more compact *cis* conformation is favored because of hydrophobic interactions. The shift from *cis* to *trans* is also greater for the anion compared to the cation, which is consistent with the asymmetry in ion hydration noted above.

Assuming that $\langle \partial E/\partial q_s \rangle_0$ is independent of solute conformation, this contribution to the total hydration free energy of the charged tetramers affects only its absolute value, not the change in free energy associated with the *cis-trans* conformational equilibrium.[2] It follows, therefore, that the adjusted Born radii, obtained from $\Delta A(\phi)$ with $q_s\langle \partial E/\partial q_s \rangle_0$ subtracted, are preferred over the unadjusted values for describing the conformational equilibrium of the charged tetramers. Continuum model predictions of $\Delta A_{hyd}(\phi)$ using the adjusted radii are compared with the simulation results in Fig. 6. The predicted conformational free energies of hydration for the anion (Fig. 6 *B*) are in excellent agreement with the simulations results. We note that the continuum model would predict an even more favorable free energy of hydrating the *trans* conformation relative to the *cis* conformation had the unadjusted Born radius ($R_- = 1.56$ Å) been used instead.

In contrast to these results, the continuum model with $R_+ = 2.42$ Å fails to capture the correct qualitative features of the conformational equilibrium for the cation (Fig. 6 *A*). In particular, the maximum in $\Delta A_{hyd}(\phi)$ is shifted from the *cis* to the *gauche* conformation ($\phi = 60°$). The predicted *gauche* maximum is a manifestation of the balance between hydrophobic and electrostatic contributions to the free energy of hydration, as shown in Fig. 7. Electrostatic contributions to ΔA_{hyd} become more negative with increasing ϕ, indicating the expected gain in favorable electrostatic interactions with water as the tetramer conformation becomes more extended. For dihedral angles between ~0° and ~60°, however, hydrophobic contributions dominate ΔA_{hyd} such that there is an initial increase in ΔA_{hyd} with increasing ϕ, followed by the maximum as electrostatic contributions gain in importance. We note that, for $R_+ = 2.82$ Å, the initial decrease in the electrostatic contribution of the hydration free energy with increasing ϕ is less pronounced. Thus the *gauche* maximum would still be present, and the agreement between the continuum model and the simulation results would have been worse. We conclude, therefore, that

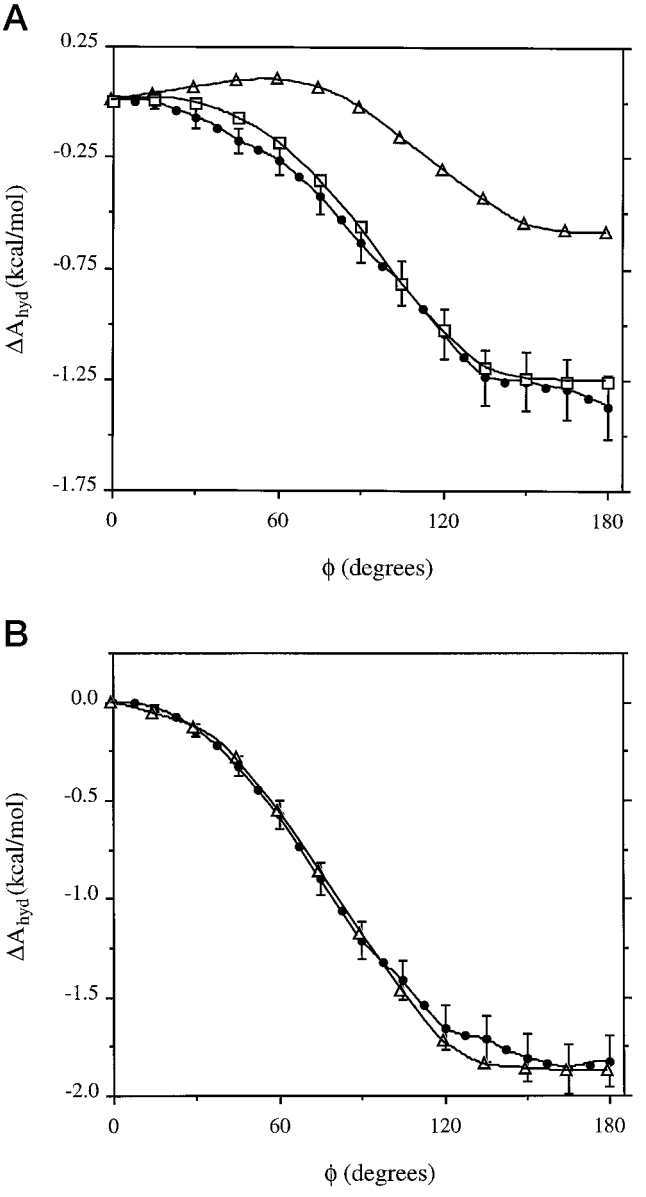

FIGURE 6 ΔA_{hyd} of the charged tetramers as a function of the backbone dihedral angle, ϕ, referenced to $\Delta A_{hyd}(\phi = 0°) = 0$. (*A*) Cationic tetramer. ●, Simulation results. △, The continuum model predictions from $R_+ = 2.42$ Å. □, The continuum model predictions from $R_+ = 2.01$ Å. (*B*) Anionic tetramer. ●, Simulation results. △, The continuum model predictions from $R_- = 1.74$ Å. Error bars on the simulation results denote one standard deviation. Hydrophobic contributions to the continuum model predictions use the vdW surface and $\gamma = 109$ cal/(mol Å^2).

a smaller value of the Born radius is needed to fit to the free energy profile for the cation in Fig. 6 *A*. We find that quantitative agreement with the simulation results is obtained with $R_+ = 2.01$ Å (see Fig. 6 *A*), but comes at the expense of a poorer prediction of the free energy charging the cation. Using $R_+ = 2.01$ Å, the continuum model predicts the free energy of charging the cation to be −76.7 kcal/mol, which is substantially more negative than -65.2 ± 0.8 kcal/mol, the value obtained after adjusting for $q_s\langle \partial E/\partial q_s \rangle_0$.

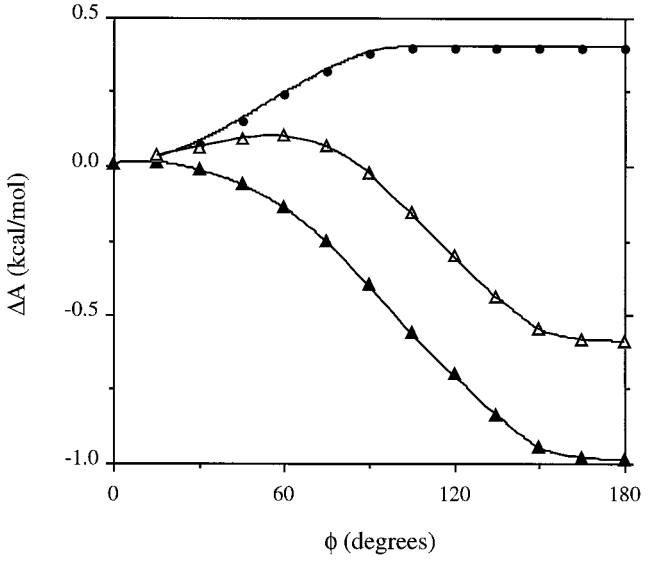

FIGURE 7 Hydrophobic and electrostatic contributions to ΔA_{hyd}, predicted using the continuum model with $R_+ = 2.42$ Å. ●, The hydrophobic contributions to the free energy. ▲, The electrostatic contributions to the free energy. △, The total free energy. Hydrophobic contributions are calculated using the vdW surface and $\gamma = 109$ cal/(mol Å^2).

To examine why the optimal R_+ is different for the charging and the conformational free energies of hydration for the cation, we consider the free energy of charging *cis*-butane. Path independence of the free energy guarantees that

$$\Delta A_{hyd}(0e \rightarrow +1e)|_{\phi=180^\circ} - \Delta A_{hyd}(0e \rightarrow +1e)|_{\phi=0^\circ} = \Delta A_{hyd}(0^\circ \rightarrow 180^\circ)|_{+1e} - \Delta A_{hyd}(0^\circ \rightarrow 180^\circ)|_{0e} \quad (18)$$

from which $\Delta A_{hyd}(0e \rightarrow +1e)|_{\phi=0^\circ} = -63.4 \pm 0.8$ kcal/mol, after subtracting $q_s\langle \partial E/\partial q_s \rangle_0$. Fitting the continuum model to this value, we obtain $R_+ = 2.46$ Å. Thus $\delta R_+ = 0.04 \pm 0.004$ Å for the *trans* to *cis* conformational change. Using an analytical approximation based on the Born equation to determine the effect of changing the Born radius on the free energy of charging the tetramer, we find the optimal value of $R_+ = 2.45$ Å for the *cis* conformation, in good agreement with the value calculated above.[3] We conclude, therefore, that changes in the Born radius on the order of 1–2% as a function of ϕ can significantly alter the conformational equilibrium of the charged tetramers. The difference between R_+ optimized to either the charging free energies of the *trans* and *cis* conformations ($R_+ = 2.42$–2.46 Å) or the *cis-trans* conformational free energy ($R_+ = 2.01$ Å) is analogous to the difference in γ values obtained from the hydration free energy and conformational free energy of the uncharged tetramer.

CONCLUSIONS

The computational efficiency of the continuum model relative to explicit water simulations makes it appealing for studying hydrated macromolecules. Moreover, the continuum model establishes a convenient framework for discussing many aspects of hydration. In this paper we compared implementations of the continuum model based on either transfer or conformational free energies of hydation. Our motivation was to assess the ability of the continuum model to describe simultaneously the transfer thermodynamics and the conformational equilibria for a collection of simple hydrophobic and amphiphilic solutes in water.

Continuum hydrophobic effects are embodied within γ, the free energy/surface area coefficient. Comparing the free energies of hydration of the *n*-alkanes to the conformational free energy profile of *n*-butane in water, we have shown that γ can differ by as much as an order of magnitude, depending on which process is modeled. Furthermore, although *n*-alkane hydration free energies are described equally well by vdW, solvent-accessible, or molecular surfaces, the vdW surface is the best choice for the conformational equilibrium of *n*-butane. These observations highlight the empirical nature of a linear relationship between surface area and hydration free energy (Eq. 10), and suggest that microscopic hydrophobic effects are richer than implied by this simple correlation.

A question that naturally follows is: To what extent can these simple linear free energy relationships be applied to the hydration of macromolecular solutes? We are currently examining the conformational behavior of longer *n*-alkanes in water to gain insight into this question (Ashbaugh, 1998). Recent simulations of the collapse of *n*-dodecane in water have led to an estimate for γ of 140 cal/(mol Å^2), based on the molecular surface area (Wallqvist and Covell, 1995, 1996). We estimate γ for the collapse of *n*-dodecane to be 110 cal/(mol Å^2) when we account for differences in the methyl group radius that was used in that study and here.[4] This value is in very good agreement with our result for *n*-butane. Thus it appears reasonable that the value of γ determined from the conformational equilibrium for *n*-butane conformation can be applied to significantly longer chain *n*-alkanes. Recent continuum modeling of alanine dipeptide conformational transitions (Marrone et al., 1996; Ösapay et al., 1996; Schmidt and Fine, 1994) and α-helix propagation (Yang and Honig, 1995a) concluded that hydrophobic contributions to these processes are negligible and that they are driven by electrostatics. However, the continuum parameters used in these studies were optimized to experimental information on transfer thermodynamics. In light of the present results, the conclusions drawn above regarding biomolecular conformational equilibrium most likely have underestimated the magnitude of the hydrophobic driving force toward collapse.

Like γ in the continuum treatment of hydrophobic effects, the Born radius in the continuum treatment of electrostatics is empirical in nature. We identified two definitions of the Born radius that can be applied to calculate charging free energies of the terminal methyl group of the cationic and anionic tetramers. The difference between these definitions is a contribution that corrects for the re-

sidual electrostatic potential of the uncharged cavity in water. It was shown that values of the Born radii accounting for this correction give a more accurate description of the conformational free energies of the charged tetramers in water. Thus we conclude that hydrophobic and electrostatic contributions are not completely decoupled, as is assumed in the continuum treatment. Indeed, a significant contribution to the free energy of ion hydration can be attributed to the hydration structure in the vicinity of an uncharged cavity. Taking this hydrophobic contribution into account in defining Born radii for the charging free energies is expected to improve the accuracy and extend the range of applicability of the continuum treatment of hydration phenomena.

Much like γ, we find that different Born radii are needed to fit the charging free energies of the *cis* and *trans* ionic tetramers, although this difference is relatively small. In contrast, the effective Born radius that fits the corresponding conformational free energy profile is significantly less than either of these two values. In particular, the Born radius of a cationic methyl group obtained from the charging free energy qualitatively fails to predict the conformational behavior of the cationic tetramer. Using a Born radius that is ~20% lower than this charging value brings the continuum conformational free energies into agreement with simulation. However, the improved conformational description comes at the expense of predicting an absolute charging free energy that is too low. We attribute the difference between the charging and conformational values of R_+ to a decrease in the optimal charging value for the *cis* and *trans* conformations of only 1.5%, which results in the observed 20% decrease in the radius that best describes the conformational equilibrium. Although this effect was observed only for the cationic solute, it should be noted that the values of R_- and R_+ depend on the assumed radius of the uncharged groups. Had a vdW radius of 2.0 Å been used instead of 1.9 Å, the optimal charging Born radii would be less. It follows that the charging value of R_+ would be in better agreement with its conformational value, and the value R_- would be in worse agreement.

In conclusion, continuum predictions of conformational equilibria in aqueous solution are extremely sensitive to small perturbations in both the optimal hydrophobic and electrostatic parameters that describe the vacuum-to-water transfer of the model solutes we examined. Not only do these perturbations lead to effective parameters that best describe hydrated conformational equilibria; they effect the balance of hydrophobic and electrostatic interactions that determine the solute conformational state. In particular, we note that hydrophobic contributions to conformational collapse are significantly underestimated by the vacuum-to-water transfer free energies.

The authors are indebted to Dr. B. L. Neal and Prof. A. M. Lenhoff for providing the software used to solve Poisson's equation via the BEM. We acknowledge Prof. R. J. Zauhar, who provided the SMART surface discretization program. HSA thanks Dr. S. Garde and Prof. R. H. Wood for many useful discussions.

Financial support from the National Aeronautics and Space Administration (NAG3–1954), the National Science Foundation (BES-9210401 and BES-9510420), and a National Science Foundation Fellowship for HSA (GER-9253850) is gratefully acknowledged.

ENDNOTES

1. The potential at zero charge appears to contribute $q_s\langle\partial E/\partial q_s\rangle_0$ to the charging free energy calculated with Eq. 4, but only $q_s\langle\partial E/\partial q_s\rangle_0/2$ to the free energy calculated with Eq. 5. Even so, we subtract the full $q_s\langle\partial E/\partial q_s\rangle_0$ from the reported charging free energies calculated with Eq. 5. The justification is that only relative differences in the electrostatic potential are meaningful. The electrostatic potential determined from a simulation is measured with respect to the bulk solvent having a reference potential of zero. When the potential is measured relative to $\langle\partial E/\partial q_s\rangle_0$ determined from simulation, however, we must subtract $\langle\partial E/\partial q_s\rangle_0$ not only from the potential at zero charge, making it effectively zero as in the continuum model, but from the potential at charge q_s as well. This is equivalent to subtracting $q_s\langle\partial E/\partial q_s\rangle_0$ from the charging free energy independent of the formula used to evaluate the charging free energy. It is easily verified for an electrically neutral system that shifting the electrostatic potential by a constant value does not affect the net free energy.

2. To determine the conformational dependence of $\langle\partial E/\partial q_s\rangle_0$, we performed additional simulations of hydrated *cis*-butane. We calculated a value of 8.3 ± 0.3 kcal/(mol *e*) for the free energy of charging, which agrees within the statistical uncertainty with the value for *trans*-butane (Table 5). The result supports the assumed conformational independence of $\langle\partial E/\partial q_s\rangle_0$.

3. The Born equation (Eq. 15) is derived for charging a spherical ion. As applied to *n*-butane, this equation neglects any effects due to the attached, uncharged propyl group on the free energy of charging the terminal methyl group, and hence has no conformational dependence. The Born equation, however, does capture the effect of changes in the Born radius. For a small perturbation in the radius of δR, the Born equation predicts a perturbation in the charging free energy of

$$\begin{aligned}\delta[\Delta A_{hyd}(0 \rightarrow q_s)] &= \delta R q_s^2/8\pi\epsilon_0 R^2(1 - 1/\epsilon_{aq}) \\ &= -8\delta R/R\ \Delta A_{hyd}(0 \rightarrow q_s)\end{aligned} \tag{19}$$

Thus a 1% increase in the radius ($\delta R/R = 0.01$) results in a 1% increase in the charging free energy.

The free energy of charging the *cis* conformation of *n*-butane obtained from simulation is $\Delta A_{hyd}(0e \rightarrow +1e)|_{\phi=0^\circ} = -63.4 \pm 0.8$ kcal/mol, after subtracting $q_s\langle\partial E/\partial q_s\rangle_0$. From the continuum model with $R_+ = 2.42$ Å, we calculate $\Delta A_{hyd}(0e \rightarrow +1e)|_{\phi=0^\circ} = -64.2$ kcal/mol. Therefore, the continuum model prediction is $\delta[\Delta A_{hyd}(0e \rightarrow +1e)] = 0.8 \pm 0.1$ kcal/mol more negative than the simulation result. Substituting $\Delta A_{hyd}(0e \rightarrow +1e)|_{\phi=0^\circ} = -64.2$ kcal/mol, $\delta[\Delta A_{hyd}(0e \rightarrow +1e)] = 0.8 \pm 0.1$ kcal/mol, and $R_+ = 2.42$ Å into Eq. 18, we calculate $\delta R_+ = 0.03 \pm 0.003$ Å. Thus the best value for R_+ in the *cis* conformation is 2.45 Å.

4. The radius of a methyl site on *n*-dodecane was assumed by Wallqvist and Covell to be 1.7 Å, which is a better estimate of the vdW radius of a lone carbon without pendant hydrogens. An uncharged carbon radius of 1.9 Å was used throughout this work. The water probe radius used in both studies was 1.4 Å. We estimate γ for the collapse of *n*-dodecane, using a radius of 1.9 Å, to be $\gamma(1.9\text{ Å}) \approx \gamma(1.7\text{ Å})(1.7\text{ Å}/1.9\text{ Å})^2 = 110$ cal/(mol Å^2). This estimate is in good agreement with γ evaluated from the conformational behavior of *n*-butane of 111 cal/(mol Å^2).

REFERENCES

Allen, M. P., and D. J. Tildesley. 1987. Computer Simulation of Liquids. Oxford University Press, Oxford.

Åqvist, J., and T. Hansson. 1996. On the validity of electrostatic linear response in polar solvents. *J. Phys. Chem.* 100:9512–9521.

Ashbaugh, H. S. 1998. The hydration of amphiphilic solutes: a theoretical and modeling perspective. Ph.D. dissertation. University of Delaware, Newark, DE.

Ashbaugh, H. S., and M. E. Paulaitis. 1996. Entropy of hydrophobic hydration: extension to hydrophobic chains. *J. Phys. Chem.* 100: 1900–1914.

Ashbaugh, H. S., and R. H. Wood. 1997. Effects of long-range electrostatic potential truncation of the free energy of ionic hydration. *J. Chem. Phys.* 106:8135–8139.

Ben-Naim, A. 1978. Standard thermodynamics of transfer. Uses and misuses. *J. Phys. Chem.* 82:792–803.

Ben-Naim, A., and Y. Marcus. 1984. Solvation thermodynamics of nonionic solutes. *J. Chem. Phys.* 81:2016–2027.

Berendsen, H. J. C., J. P. M. Postma, W. F. van Gunsteren, and J. Hermans. 1981. Interaction models of water in relation to protein hydration. *In* Intermolecular Forces: Proceedings of the Fourteenth Jerusalem Symposium on Quantum Chemistry and Biochemistry. B. Pullman, editor. D. Reidel Publishing Company, Dordrecht, the Netherlands. 331–342.

Born, M. 1920. Volumen un Hydrationwärme der Ionen. *Z. Phys.* 1:45–48.

Chothia, C. 1974. Hydrophobic bonding and accessible surface area in proteins. *Nature.* 248:338–339.

Connolly, M. L. 1981. Molecular Surface Program: Program 429. *Quantum Chemistry Program Exchange Bull.* 1:75.

Connolly, M. L. 1983. Analytical molecular surface calculation. *J. Appl. Crystallogr.* 16:548–558.

De Leeuw, S. W., J. W. Perram, and E. R. Smith. 1980. Simulation of electrostatic systems in periodic boundary conditions. I. Lattice sums and dielectric constant. *Proc. R. Soc. Lond.* A373:27–56.

Figueirido, F., G. S. Del Buono, and R. M. Levy. 1994. Molecular mechanics of electrostatic effects. *Biophys. Chem.* 51:235–241.

Garde, S., G. Hummer, and M. E. Paulaitis. 1996. Hydrophobic interactions: conformational equilibria and the association of non-polar molecules in water. *Faraday Discuss. Chem. Soc.* 103:125–139.

Garde, S., G. Hummer, and M. E. Paulaitis. 1998. Free energy of hydration of a molecular ionic solute: tetramethyl ammonium ion. *J. Chem. Phys.* 108:1552–1561.

Hermann, R. B. 1972. Theory of hydrophobic bonding. II. The correlation of hydrocarbon solubility with solvent cavity surface area. *J. Phys. Chem.* 76:2754–275.

Honig, B., and A. Nicholls. 1995. Classical electrostatics in biology and chemistry. *Science.* 268:1144–1149.

Horvath, D., D. van Belle, G. Lippens, and S. J. Wodak. 1996. Development and parameterization of continuum solvent models. 1. Models based on the boundary element method. *J. Chem. Phys.* 104:6679–6695.

Hummer, G., S. Garde, A. E. García, M. E. Paulaitis, and L. R. Pratt. 1998. Pressure denaturation of proteins. *Proc. Natl. Acad. Sci. USA.* 95: 1552–1555.

Hummer, G., S. Garde, A. E. García, A. Pohorille, and L. R. Pratt. 1996a. An information theory model of hydrophobic interactions. *Proc. Natl. Acad. Sci. USA.* 93:8951–8955.

Hummer, G., L. R. Pratt, and A. E. García. 1995. Hydration free energy of water. *J. Phys. Chem.* 99:14188–14194.

Hummer, G., L. R. Pratt, and A. E. García. 1996b. Free energy of ionic hydration. *J. Phys. Chem.* 100:1206–1215.

Hummer, G., L. R. Pratt, A. E. García, B. J. Berne, and S. W. Rick. 1997. Electrostatic potentials and free energies of solvation of polar and charged molecules. *J. Phys. Chem. B.* 101:3017–3020.

Hummer, G., D. M. Soumpasis, and M. Neumann. 1994. Computer simulation of aqueous Na-Cl electrolytes. *J. Phys. Cond. Matter.* 6:A141–A144.

Hummer, G., and A. Szabo. 1996. Calculation of free-energy differences from computer simulations of initial and final states. *J. Chem. Phys.* 105:2004–2010.

Hunter, R. J. 1987. Foundations of Colloid Science. Oxford University Press, Oxford.

Israelachvili, J. 1992. Intermolecular and Surface Forces. Academic Press, London.

Jackson, J. D. 1975. Classical Electrodynamics. Wiley, New York.

Jackson, R. M., and M. J. E. Sternberg. 1993. Protein surface area defined. *Nature.* 366:638.

Jackson, R. M., and M. J. E. Sternberg. 1994. Application of scaled particle theory to model the hydrophobic effect: implication for molecular association and protein stability. *Protein Eng.* 7:371–383.

Jayaram, B., R. Fine, K. Sharp, and B. Honig. 1989. Free energy calculations of ion hydration: an analysis of the Born model in terms of microscopic simulations. *J. Phys. Chem.* 93:4320–4327.

Jorgensen, W. L. 1982. Mote Carlo simulation of *n*-butane in water. Conformational evidence for the hydrophobic effect. *J. Chem. Phys.* 77:5757–5765.

Jorgensen, W. L., and J. K. Buckner. 1987. Use of statistical perturbation theory for computing solvent effects on molecular conformation. Butane in water. *J. Phys. Chem.* 91:6083–6085.

Jorgensen, W. L., J. D. Madura, and C. J. Swenson. 1984. Optimized intermolecular potential functions for liquid hydrocarbons. *J. Am. Chem. Soc.* 106:6638–6646.

Kalko, S. G., G. Sesé, and J. A. Padró. 1996. On the effects of truncating the electrostatic interactions: free energies of ion hydration. *J. Chem. Phys.* 104:9578–9585.

Kaminski, G., E. M. Duffy, T. Matsui, and W. L. Jorgensen. 1994. Free energies of hydration and pure liquid properties of hydrocarbons from the OPLS all-atom model. *J. Phys. Chem.* 98:13077–13082.

Kauzmann, W. 1959. Some factors in the interpretation of protein denaturation. *Adv. Protein Chem.* 14:1–63.

Lee, B., and F. M. Richards. 1971. Protein structures: estimation of static accessibility. *J. Mol. Biol.* 55:379–400.

Lüdemann, S., R. Abseher, H. Schreiber, and O. Steinhauser. 1997. The temperature dependence of hydrophobic association in water. Pair versus bulk hydrophobic interactions. *J. Am. Chem. Soc.* 119:4206–4213.

Lüdemann, S., H. Schreiber, R. Abseher, and O. Steinhauser. 1996. The influence of temperature on pairwise hydrophobic interactions of methane-like particles: a molecular dynamics study of free energy. *J. Chem. Phys.* 104:286–295.

Marrone, T. J., M. K. Gilson, and J. A. McCammon. 1996. Comparison of continuum and explicit models of solvation: potentials of mean force for alanine dipeptide. *J. Phys. Chem.* 100:1439–1441.

McAuliffe, C. 1966. Solubility in water of paraffin, cycloparafin, olefin, acetylene, cycloolefin, and aromatic hydrocarbons. *J. Phys. Chem.* 70: 1267–1275.

Nakamura, H. 1996. Role of electrostatic interactions in proteins. *Q. Rev. Biophys.* 29:1–90.

Neal, B. L. 1997. Molecular thermodynamic properties of aqueous protein solutions. Ph.D. dissertation. University of Delaware, Newark, DE.

New, M. H., and B. J. Berne. 1995. Molecular dynamics calculation of the effect of solvent polarizability on the hydrophobic interaction. *J. Am. Chem. Soc.* 117:7172–7179.

Ösapay, K., W. S. Young, D. Bashford, C. L. Brooks, III, and D. A. Case. 1996. Dielectric continuum models for hydration effects on peptide conformational transitions. *J. Phys. Chem.* 100:2698–2705.

Owicki, J. C., and H. A. Scheraga. 1977. Preferential sampling near solutes in Monte Carlo calculations on dilute solutions. *Chem. Phys. Lett.* 47:600–602.

Pangali, C., M. Rao, and B. J. Berne. 1979. A Monte Carlo simulation of the hydrophobic interaction. *J. Chem. Phys.* 71:2975–2981.

Payne, V. A., N. Matubayasi, L. R. Murphy, and R. M. Levy. 1997. Monte Carlo study of the effect of pressure on hydrophobic association. *J. Phys. Chem. B.* 101:2054–2060.

Pitarch, J., V. Moliner, J. Pascual-Ahuir, E. Silla, and I. Tuñón. 1996. Can hydrophobic interactions be correctly reproduced by the continuum models? *J. Phys. Chem.* 100:9955–9959.

Pratt, L. R., and D. Chandler. 1977. Theory of the hydrophobic effect. *J. Chem. Phys.* 67:3683.

Pratt, L. R., G. Hummer, and A. E. García. 1994. Ion pair potentials-of-mean-force in water. *Biophys. Chem.* 51:147–165.

Pratt, L. R., G. J. Tawa, G. Hummer, and A. E. García. 1997. Boundary integral methods for the Poisson equation of continuum dielectric solvation models. *Int. J. Quant. Chem.* 64:121–141.

Rank, J. A., and D. Baker. 1997. A desolvation barrier to hydrophobic cluster formation may contribute to the rate-limiting step in protein folding. *Protein Sci.* 6:347–354.

Rashin, A. A. 1990. Hydration phenomena, classical electrostatics, and the boundary element method. *J. Phys. Chem.* 94:1725–1733.

Reynolds, J. A., D. B. Gilbert, and C. Tanford. 1974. Empirical correlation between hydrophobic free energy and aqueous cavity surface area. *Proc. Natl. Acad. Sci. USA.* 71:2925–2927.

Richards, F. M. 1977. Area, volumes, packing, and protein structure. *Annu. Rev. Biophys. Bioeng.* 6:151–176.

Rick, S. W., and B. J. Berne. 1994. The aqueous solvation of water: a comparison of continuum methods with molecular dynamics. *J. Am. Chem. Soc.* 116:2949–2954.

Rogers, N. K. 1986. The modelling of electrostatic interactions in the function of globular proteins. *Prog. Biophys. Mol. Biol.* 48:37–66.

Rosenberg, R. O., R. Mikkilineni, and B. J. Berne. 1982. Hydrophobic effect on chain folding. The *trans* to *gauche* isomeriztion of *n*-butane in water. *J. Am. Chem. Soc.* 104:7647–7649.

Schmidt, A. B., and R. M. Fine. 1994. A CFF91-based continuum solvation model: solvation free energies of small organic molecules and conformations of the alanine dipeptide in solution. *Mol. Sim.* 13:347–365.

Sitkoff, D., N. Ben-Tal, and B. Honig. 1996. Calculation of alkane to water solvation free energies using continuum solvent models. *J. Phys. Chem.* 100:2744–2752.

Sitkoff, D., K. A. Sharp, and B. Honig. 1994. Accurate calculation of hydration free energies using macroscopic solvent models. *J. Phys. Chem.* 98:1978–1988.

Skipper, N. T., C. H. Bridgeman, A. D. Buckingham, and R. L. Mancera. 1996. Computer simulation studies of the hydration and aggregation of simple hydrophobic molecules. *Faraday Discuss. Chem. Soc.* 103: 141–150.

Smith, D., and A. D. J. Haymet. 1993. Free energy, entropy, and internal energy of hydrophobic interactions: computer simulations. *J. Chem. Phys.* 98:6445–6454.

Straatsma, T. P., and H. J. C. Berendsen. 1988. Free energy of ionic hydration: analysis of a thermodynamic integration technique to evaluate free energy differences by molecular dynamics simulations. *J. Chem. Phys.* 89:5876–5886.

Tobias, D. J., and C. L. Brooks, III. 1990. The thermodynamics of solvaphobic effects: a molecular dynamics study of *n*-butane in carbon tetrachloride and water. *J. Chem. Phys.* 92:2582–2592.

van Belle, D., and S. J. Wodak. 1993. Molecular dynamics study of methane hydration and methane association in a polarizable water phase. *J. Am. Chem. Soc.* 115:647–652.

Wallqvist, A., and B. J. Berne. 1995a. Computer simulation of hydrophobic hydration forces on stacked plates at short range. *J. Phys. Chem.* 99: 2893–2899.

Wallqvist, A., and B. J. Berne. 1995b. Molecular dynamics study of the dependence of water solvation free energy on solute curvature and surface area. *J. Phys. Chem.* 99:2885–2892.

Wallqvist, A., and D. G. Covell. 1995. Free-energy cost of bending *n*-dodecane in aqueous solution. Influence of the hydrophobic effect and solvent exposed area. *J. Phys. Chem.* 99:13118–13125.

Wallqvist, A., and D. G. Covell. 1996. On the origins of the hydrophobic effect: observations from simulations of *n*-dodecane in model solvents. *Biophys. J.* 71:600–608.

Yang, A., and B. Honig. 1995a. Free energy determinants of secondary structure formation. I. α-Helices. *J. Mol. Biol.* 252:351–365.

Yang, A., and B. Honig. 1995b. Free energy determinants of secondary structure formation. II. Antiparallel β-sheets. *J. Mol. Biol.* 252:366–376.

Yoon, B. J., and A. M. Lenhoff. 1990. A boundary element method for molecular electrostatics with electrolyte effects. *J. Comp. Chem.* 11: 1080–1086.

Young, W. S., and C. L. Brooks, III. 1997. A reexamination of the hydrophobic effect: exploring the role of the solvent model in computing the methane-methane potential of mean force. *J. Chem. Phys.* 106: 9265–9269.

Zauhar, R. J. 1995. SMART: A solvent-accessible triangulated surface generator for molecular graphics and boundary element applications. *J. Comput. Aided Mol. Design.* 9:149–159.

Zauhar, R. J., and R. S. Morgan. 1985. A new method for computing the macromolecular electric potential. *J. Mol. Biol.* 186:815–820.

Zichi, D. A., and P. J. Rossky. 1986. Molecular conformation equilibria in liquids. *J. Chem. Phys.* 84:1712–1723.

Zwanzig, R. W. 1954. High-temperature equation of state by a perturbation method. 1. Nonpolar gases. *J. Chem. Phys.* 22:1420–1426.